POSITION OF THE SOURCE OF DAYLIGHT HIGH-LATITUDE MAGNETIC PULSES IN THE MAGNETOSPHERE ACCORDING TO DMSP SATELLITE DATA

© 2025 V. V. Safargaleev

Pushkov Institute of Terrestrial Magnetism, Ionosphere and Radio Wave Propagation RAS, St. Petersburg Department, St. Petersburg, Russia

e-mail: Vladimir.safargaleev@pgia.ru

Received March 21, 2024

Revised June 27, 2024

Accepted July 25, 2024

Abstract. Daytime high-latitude geophysical phenomena provide a ground-based observer with information about processes at the daytime magnetopause and/or in adjacent magnetospheric domains. It is assumed that these phenomena are initiated by changes in the parameters of the interplanetary medium and therefore can be used as a tool for studying the ways in which solar wind energy penetrates through the magnetopause. Such phenomena include magnetic impulses, which are an isolated train of damped oscillations of 2-3 bursts with a repetition period of 8-12 minutes. Using data from the Scandinavian network of magnetometers IMAGE, eight magnetic impulse events were studied for which DMSP satellites flew over the observation area during, shortly before and immediately after the pulse, crossing the boundaries of several domains. Based on ground-based and satellite data, it has been shown that the downward field-aligned current associated with the impulses is located away from the magnetopause. This means that the impulse cannot be considered as an ionospheric trace of a reconnected magnetic flux tube (flux transfer event, FTE) and/or as a traveling convection vortex (TCV). Using more statistics, it has been established that the pulse is preceded by noticeable changes in the *By* and *Bz* components of the IMF, while the contribution to the generation of the impulse from the pressure jump and solar wind speed, as well as the *Bx* component of the IMF, is not obvious. A possible scenario for the initiation of a magnetic pulse by IMF variations is discussed.

Keywords: *magnetic impulses, magnetospheric domains, equivalent ionospheric currents*

DOI: 10.31857/S00167940250612e5

1. INTRODUCTION

A key link in the formation of space weather is the entry of energy and matter from the solar wind into the magnetosphere. It is widely accepted that the penetration of energy and matter occurs predominantly through that part of the daily magnetopause, which is "resting" on the high-latitude ionosphere in the vicinity of the noon meridian by the soles of the geomagnetic field force lines forming it. This makes the monitoring of processes in the casp and in the magnetospheric domains adjacent to the magnetopause - the low-latitude plasma layer (*llbl*), the boundary plasma layer (*bps*), and the central plasma layer (*cps*) - an important element in the study of the mechanisms of the realization of solar-terrestrial relations. The coupling of these regions with the high-latitude ionosphere allows us to study the process of interaction of the solar wind with the magnetosphere through a number of daytime phenomena observed from the Earth's surface. Based on the DMSP satellite data ([Newell and Meng, 1992]), it can be stated that during daytime hours and at different levels of geomagnetic activity, the IMAGE network magnetic stations located on the Svalbard Archipelago, off its southern coast and on Bear Island "pass" under the projection of all the above-mentioned magnetospheric formations.

Since the 1980s, *magnetic impulse events (*MIEs) have been considered as one of such terrestrial phenomena. MIEs are isolated damped burst-like perturbations of the magnetic field registered by ground-based magnetometers at the Caspian latitude (see, for example, [Lanzerotti el al., 1986]). At the initial stage of research, interest in this phenomenon was motivated by the fact that MIEs were interpreted as a ground-based sign of sporadic reconnection at the daily magnetopause - so-called flux transfer events, FTEs ([Goertz et al., 1985], [Lanzerotti el al., 1986] and references therein). As an alternative to reconnection, Sibeck [1992] proposed surface waves at the daytime magnetopause generated as a result of a slow shock front impacting the magnetosphere, at which the plasma pressure changes rapidly (*sudden impulses*, SI).

During daytime hours in the European part of the eastern hemisphere, the magnetopause (the boundary between closed and open force lines) is statistically projected to the northern part of Svalbard ([Newell and Meng, 1992]), where there is no dense network of observations. Cases where the boundary descends so low that it falls, for example, within the field of view of the STARE radar over the northern coast of Norway ([Goertz et al., 1985]) are exotic. Magnetic pulses are rare but not exotic phenomena. Therefore, the hypothesis of Sibeck et al., 2003 that magnetic pulses reflect in the ionosphere the development of the Kelvin-Helmholtz instability at the convection reversal boundary, which is considered to be the inner *llbl* boundary, seems to be closer to reality. Note that the work of Clauer et al. [1997], referred to by Sibeck et al. [2003], was devoted to the generation of pulsations with a period close to the period of the bursts in the magnetic pulse. However, using two cases as examples, Yahnin et al. [1997] showed that the longitudinal current

associated with MIEs is located deeper in the magnetosphere than the inner boundary of *llbl*, namely, inside the central plasma layer, *cps.* Using a different terminology for rash regions, Vorobyev [2004] concluded that propagating convective vortices (TCVs), which are categorized as "magnetic pulses", are generated in the near-pole part of the diffuse auroral zone, that is, as deep in the magnetosphere. The question in which magnetospheric domains the source of MIEs is located is still debatable today.

The probability of detecting magnetic pulses has a maximum in the interval 08-10 MLT (05-07 UT for high-latitude stations of the IMAGE network), and, as noted in [Vorobyov et al., 1993], their occurrence is not connected with the rotation of the Bz-component of the *MIEs* to the south. In most of the cases studied in this work, magnetic pulses were also observed at middle and low latitudes, which, in the authors' opinion, indicates the deformation of the daytime magnetosphere as the cause of the generation of MIEs. The same conclusion was reached in [Yahnin et al., 1995] based on the analysis of a series of several events observed during one three-hour interval. Four cases in which SI-initiated TCV events could be attributed to Kelvin-Helmholtz instabilities at the *llbl* inner boundary are presented in [Sibeck et al., 2003].

One case of TCV caused by a sudden pulse is comprehensively investigated in the recent work of Kim et al. [2017]. As noted above, TCV is categorized as a magnetic pulse. TCV and its associated phenomena have been observed by a large number of instruments both on the Earth's surface (magnetometer, radars, camera, and SCANDI full-sky scanning interferometer) and on satellites (NOAA and DMSP). It was shown that the pulse is accompanied by an increase in rashes, an increase in plasma temperature in the ionosphere, and a spike in magnetic activity in the Hertz range. The authors were also able to isolate its effect in the thermosphere. It is noted that the center of the convective vortex was located near the casp. However, interpretation of the bright spot among other forms of auroras as a result of spills from the caspas seems to be poorly justified.

The interpretation of magnetic pulses within the SI framework does not agree with the results of Bering et al. [1990], according to which magnetic pulses are associated with strong changes in the direction of the IMF at the background of almost constant solar wind pressure. According to statistical studies by Konik et al. [1994], 50-70% of magnetic pulse events are associated with variations of the *By*- and *Bz*-components of the MMP, while only 15-30% of the events followed changes in the solar wind pressure.

Later Moretto et al. [2004] noted that pulses appear more frequently at high-speed solar wind flow, but in general, pulse generation is determined by a wide range of conditions in the interplanetary medium.

It is known that a magnetic barrier is formed in the transition region as a result of the solar wind running into the magnetopause, in which the magnetic field and concentration (plasma

pressure) are interrelated. Variations in the MMP produce variations in plasma pressure, which, like the SC or SI, and affect the magnetopause. As a result, the magnetopause becomes a source of magnetosonic-type secondary waves. This qualitative reasoning is supported by numerical simulation results ([Lin et al., 1996]). The authors propose to consider these secondary waves as the cause of high-latitude magnetic pulses. A similar assumption was made in [Vorobjev et al., 1999].

MIEs research peaked in the late 20th and early 21st centuries. However, the question of the nature of magnetic pulses (or TCV as a form of magnetic pulse) remains debatable even today. The purpose of this paper is to propose answers to the following two fundamentally important questions for understanding the nature of MIEs. The first question that arises when trying to relate magnetic pulse events to the processes of interaction of the solar wind with the magnetopause is in which magnetospheric domain their source is located. The answer to this question will show how far from the magnetopause the source of the magnetic pulse is located. The second question is which interplanetary medium parameters variations can be associated with the launching of a magnetic pulse, and how these variations lead to the appearance of the source of magnetic pulses in the magnetospheric domains distant from the magnetopause.

2. APPARATUS AND METHODOLOGY

The search for magnetic pulses was carried out using data from the IMAGE network of magnetometers. The list of stations used for this purpose (as well as three low-latitude stations) with code, geographic and geomagnetic coordinates is given in Table 1. The time interval of the search was 06:00− 12:00 UT, which for the IMAGE stations listed in Table 1 corresponds to an interval of ~ 08:30− 14:30 MLT. The aforementioned interval of the most likely detection of MIEs lies inside the search interval.

Table 1.

DMSP (*Defense Meteorological Satellite Program*) satellites fly at an altitude of 840 km from the Earth's surface in circumpolar orbits with an orbital period of 101 minutes, which gives a satellite velocity of about 7.5 km/sec. At this speed, the satellites fly over Svalbard for ~ 2 min. With pulse durations of 5 to 25 min, there is a non-zero probability of finding events where the satellite flies over stations during the pulse, not just before or after it. The satellites are equipped, in particular, with a zenith-directed particle detector (ten-channel spectrometer SSJ/4), which performs measurements of ejected particles in the energy range from 30 eV to 30 keV with a *temporal* resolution of 1 s. The automatic algorithm proposed in [Newell et al., 1991] was used to determine the boundaries of auroral intrusions. The algorithm has been validated in a number of studies for pre-midday rashes (see, for example, [de la Beaujardiere et al.,1993]. In particular, good

agreement between the automatic and visual (spectrogram-based) method of determining the *bps/cps* boundary is noted. Note also that according to statistical studies (see Fig. 2 in [Newell and Meng, 1992]), in the 9− 12 MLT interval, the boundaries of magnetospheric domains are oriented predominantly along the geomagnetic latitude. The magnetic pulse events analyzed in this work belong to this MLT interval.

DMSP data in the form of spectrograms indicating domain boundaries were obtained *on-line* at the J. Hopkins University website (Internet address http://sd-www.jhuapl.edu/Aurora/spectrogram/index.html). The spectrograms show the coordinates of the subsatellite point (see, for example, Fig. 2*a*), from which the projection of the satellite along the force line to the height of the *E-layer of* the ionosphere was calculated at a known satellite height. For such heights, it is sufficient to use only the IGRF model of the force line in the projection. Further in all figures the projection of the satellite trajectory at a height of 100 km is given. At the beginning of the study, spectrograms were available until 2015.

To clarify the position of the "sole" of the longitudinal current, with the occurrence of which we associate magnetic pulses (see further Section 3), the 1-D and 2-D intensity distribution of the ionospheric equivalent current over the IMAGE network was calculated. The calculation was performed *on-line* at the network site using the ECLAT program. The value of the geomagnetic field in the interval immediately before the onset of the magnetic pulse was taken as baseline. With this approach, the distribution of the equivalent current reflects the current perturbation, the magnetic effect of which is the magnetic pulse. To minimize the influence of non-magnetic pulse perturbations, we analyzed mostly isolated events, i.e., events with a relatively quiet geomagnetic prehistory. Even in these cases, due to the indistinct beginning of the magnetic pulse, the error in its determination was ±2 minutes. As a consequence, when further comparing the pulse with the variations of the interplanetary medium parameters near the frontal point of the shock front, we could not obtain reliable statistics on such an important parameter as the delay time of the magnetosphere response in the form of MIEs to the MMP changes.

To analyze the situation in the interplanetary medium, we used data from the WIND and ACE satellites monitoring the solar wind at a great distance from the Earth, as well as from the THEMIS (*Time History of Events and Macroscale Interactions during Substorms*) satellites at intervals when the satellites were outside the magnetosphere on the Sun's side. When comparing with magnetic pulses, the time of perturbation propagation from the satellite to the frontal point at the shock front was taken into account. The coordinates of the satellites, as well as their distance to the shock front, were estimated using the *4D Orbit Viewer* service (https://sscweb.gsfc.nasa.gov/tipsod/).

In some cases, we had to resort to the OMNI service (https://cdaweb.gsfc.nasa.gov/index.html/), which recalculates the perturbation in the solar wind to the shock frontal point online. Having in mind the statistical studies of Ridley [2000], which showed that the uncertainty of recalculation by the OMNI service can be 8-25 min, the analysis of direct satellite measurements was preferred.

Magnetic pulses are not an exceptional phenomenon. According to [Vorobyev et al., 1993], on average 0.5 pulses are detected per day. The experience of this article gives a smaller figure: 2− 4 events per month. Strict selection criteria (successful DMSP satellite overflights and quiet geomagnetic pulse prehistory) led to the fact that only 8 cases were analyzed jointly with satellite measurements in the period 2010 - 2014. Section 3 provides a detailed description of two cases. For the analysis of magnetic pulses in the context of the situation in the interplanetary environment, the database amounted to 22 cases. The results of this analysis are given in Section 4.

3. POSITION OF THE MAGNETIC PULSE SOURCE RELATIVE TO THE BOUNDARIES OF MAGNETOSPHERIC DOMAINS

This section provides a detailed analysis of two of the eight events for which data on the nature of the eruptions over the observing region are available. The use of satellite data allowed us to approximate the position of the IMAGE stations and the inferred source of the pulse relative to the boundaries of the magnetospheric domains.

3.1 Magnetic pulse 05.03.2013. Source in the form of a current layer at the bps/cps boundary

Fig. 1.

Pulse recorded at the meridional chain of NAL-SOD stations of the IMAGE network at about 06:09 UT on March 5, 2013. The change in the shape of the pulse can be traced in Fig. *1a*. In the top three magnetograms of the stations located in Svalbard and also at the HOP station south of Svalbard, the pulse begins with the increase of the *X*-component of the geomagnetic field. Hereinafter we will call such deviations as positive variation meaning that the deviation is positive with respect to the field before the beginning of the pulse. The positive variation is caused by the intensification of the equivalent ionospheric current of the eastward direction. In the magnetograms of the stations located south of Svalbard (BJN, SOR and SOD), the pulse begins as an excursion of the *X*-component towards the decreasing direction (negative variation), which corresponds to the amplification of the westward electrojet. In the following, for brevity, we will omit the characterization "perturbed" with respect to the magnetic field, ionospheric and longitudinal currents, keeping in mind that we are talking about perturbed values of these parameters rather than absolute values.

The distribution of ionospheric equivalent currents corresponding to a magnetic pulse is shown in Fig. 1 *b* and *c*. (Color figures are available in the electronic version of the paper). Recall that the equivalent currents flow only in the ionospheric plane (presumably at a height of 100 km) and create on the Earth's surface the same magnetic field as the real system of ionospheric currents. The system of equivalent currents is not a real current system because it does not include longitudinal currents.

In the diagram in Fig. 1*b*, each vertical profile reflects the current distribution along the meridian averaged over a 10-second interval. Positive values correspond to the current of the eastern direction. In the color figure in the electronic version of the paper, the intensity of the eastward electrojet is conveyed by colors ranging from green to brown. At the moment of the pulse onset at 06:09 UT, the transition region from the westward to the eastward electrojet was located between the HOP and BJN stations (Fig. 1*b*). In the colored figure, the location where the reversal of the current direction from east to west is clearly visible on as the transition from red colors to blue colors through green. The gray horizontal lines show the latitudes of the stations.

On the 2D map of the equivalent current distribution, the ECLAT program identifies three focuses of the clockwise-twisted vortex (Fig. 1*c*). The direction and magnitude of the currents are shown by vectors. Due to poor spatial resolution, the arrows at the ends of some vectors appear as thickenings. The results of the calculation of the 2-D current distribution in the region from the mainland (SOR station) to the pole should not be trusted unconditionally, since in these latitudes the magnetometer network is less dense than on the mainland. Nevertheless, the position of the vortex center agrees with the place of change of polarity of the magnetic pulse on the magnetograms and diagram (Fig.1*a*, *b*), and the vortex character of the ionospheric currents associated with magnetic pulses was already paid attention to at the initial stage of investigation of these phenomena (see, for example, the work [Friis-Christensen et al., 1988]).

According to, for example, [Lyatsky and Maltsev, 1983], in the region where the ionospheric current changes direction from east to west, the foot of the *field-aligned current* (FAC) should be located. On 2D maps of the equivalent ionospheric current calculated using the ECLAT program, the trace of the localized longitudinal current flowing into the ionosphere is often associated with the center of the current vortex twisted clockwise (e.g., [Amm et al., 2002] and [Palin et al., 2016]), which is also the case in the considered case. Formally, the magnetic pulse is a product of approximately simultaneous intensification of the eastern and western jets. We propose to consider as a "source" not the eastern and western jets separately, but the longitudinal current generating them together. Thus, the determination of the location of the source of the pulse in the magnetosphere is reduced to the determination of the spallation regions (magnetospheric

domains), within or on the boundary of which there is a current reversal region and/or the center of the current vortex.

Fig. 2.

Fig. 2*a* shows the spectrogram of electron and ion spikes registered by the DMSP F16 satellite during its flyby over the observation region just after the amplitude of the magnetic pulse reached its maximum value (arrow in Fig. 1*a*). During the flyby, the satellite crossed the boundary between the *cps* and *bps* outbursts twice. Note that the satellite made measurements around 09:00 MLT, so that, according to [de la Beaujardiere et al.,1993], the automatic boundary detection algorithm can be trusted.

In Fig. 2*b*, the satellite trajectory is projected (along the force line of the geomagnetic field) into the ionosphere at an altitude of 100 km. At this altitude, the ECLAT program calculates equivalent currents. The *bps* crossing points are marked with gray crosses. The dashed lines passing through the crosses are the geomagnetic latitude. It was noted in Section 2 that in this MLT sector, the *bps* boundaries are oriented along the geomagnetic latitude. Thus, the dashed lines show the *bps* boundaries outside the satellite trajectory.

The square in Fig. 2*b* marks the position of the vortex center located at meridian 22°E, along which the diagram in Fig. 1*b* was plotted. This and other centers are located along the equatorial *bps/cps* boundary. It can be assumed that in the considered case, the longitudinal current had the form of a strip and flowed at or near the *bps/cps* boundary. Thus, the source of the magnetic pulse was located inside the magnetosphere, at a distance from the magnetopause and *llbl*, which does not allow us to relate the magnetic pulse to reconnection events at the magnetopause or to the Kelvin-Helmholtz instability in the convection reversal region ([Clauer et al., 1997]).

3.2 Magnetic pulse on 21.04.2010. The satellite passage along the current layer.

The magnetic pulse was registered at 06:45 UT (Fig. 3*a*). The analysis was carried out according to the same scheme as in the previous case. We present this event in the paper for the following reason.

Fig. 3.

In the map of 2D current distribution (Fig. 3*c*), the ECLAT program shows that the vortex has a fine structure in the form of several focuses. The westernmost focus is located approximately at the same place where the current direction is reversed in the diagram (Fig. 3*b*). The vortex center also had a fine structure in the previous case (Fig. 1*c*). However, then the satellite trajectory passed away from the center. In the considered case, the satellite flew directly over a series of focuses (squares in Fig. 3*d*), while being in the region of spills from the *cps* in Fig. 3*d*).

The lower panel of the spectrogram in Fig. 3*d* shows that the ionic precipitates over the vortex centers were sporadic in nature. As in the previous case, the vortex was clockwise twisted, indicating the presence of an inward flowing (ions moving into the ionosphere) longitudinal current at its center. In light of this, we interpret the sporadicity of ionic precipitations as a sign of several fibers at the longitudinal current generating a fine structure in the center of the vortex.

We analyzed 8 events according to this scheme. In four cases, the source (more precisely, the center of the vortex of equivalent ionospheric currents) was located inside the central plasma layer (*cps*), in one case inside the boundary plasma layer (*bps*), and in three cases near the boundary between *bps* and *cps.* The analysis indicates that MIEs are neither a flux transfer event at the magnetopause due to reconnection (*FTE* events) nor a Kelvin-Helmholtz instability developing at the inner *llbl* boundary that generates propagating convection vortices in the ionosphere (*TCV* events). In the next section, the emergence of magnetic pulses is discussed in the context of changes in the interplanetary medium. In the Discussion section, building on the results of Sections 3 and 4, a possible mechanism for magnetic pulse generation will be proposed.

4. MAGNETIC PULSES IN THE CONTEXT OF DEVELOPMENTS IN THE INTERPLANETARY ENVIRONMENT

The statistics on this issue are more extensive, since the selection of events did not need to be limited to successful flybys of low-orbit DMSP satellites.

The results of the analysis are summarized in Table 2. The first three columns contain the number, date and time of the magnetic pulse. In the fourth column, the amplitude of variation of the solar wind pressure is given. Column 5− contains the amplitude of variation of the *X*-component of the geomagnetic field variation at low-latitude observatories. The step-like variation at equatorial stations is traditionally considered to be a sign of the compression of the daytime magnetosphere at the time of SI. In column 6− the relative changes of the x-component of the solar wind speed. The + sign indicates that the velocity has increased. We classify changes as zero if the velocity changed by less than 5 km/s. Columns 7− 9 summarize the values of the MMP components. The symbol 0.5/3.3 means that this component increased from + 0.5 to + 3.3 nTL. The symbol X is used when the component did not change or changed at the level of fluctuations (less than 0.5 nTl).

For the eight DMSP satellite flyby events, column 10 indicates the name of the magnetospheric domain where, in our opinion, the source of the magnetic pulse was located. For example, the symbol *bps/cps* means that the source is located near the boundary between these domains. These events are placed at the beginning of Table 2.

Table 2.

It was noted in the Introduction that the generation of magnetic pulses is not determined by a single factor, but by a wide range of conditions in the interplanetary medium ([Moretto et al., 2004]). We came to the same conclusion from the results of our studies. The above is demonstrated by Fig. 4. Here the magnetic pulse is considered in the context of measurements on the THB satellite. The satellite was located on the Sun-Earth line at a relatively small (compared to the ACE and WIND satellites) distance from the shock front (~ 642000 km, as given by the *4D Orbit Viewer* service). At a solar wind speed of 340 km/s, the propagation time of the solar wind inhomogeneity from the satellite to the shock wave is 31 min. This time was taken into account when comparing satellite and ground data.

Fig. 4.

In Fig. 4, the variations of the MMP, velocity, and pressure of the solar wind at the THB and WIND satellites are given in recalculation of the shock front. The interval when a magnetic pulse was observed on the IMAGE network is highlighted in gray (see Fig. *3a* for this event). About 4− 5 min before the onset of the pulse, the *Bx* - and *Bz* -components of the MMP change rapidly toward negative values. The *By*-component also changes rapidly in the same direction, but by a smaller value. The MMP changes are accompanied by a rapid increase in the solar wind speed atΔ Vx ~ 20 km/s (6%).

In contrast to the magnetic field and velocity, the solar wind pressure does not show a step-like variation on the satellites either near the shock front or far from it (solid and dashed lines in Fig. 4, respectively), characteristic of the phenomenon known in the literature as sudden impulse (SI). Nevertheless, the variation of the *X* component at the AAE equatorial station, ΔX, resembles in shape (but not in magnitude) the magnetospheric response to SI (Fig. 4, bottom panel). According, for example, to [Safargaleev et al., 2002], the typical magnitude of the geomagnetic response to SI at equatorial stations is $\Delta X \sim 40$ nTL, i.e., 10 times larger. At the time resolution of the AAE data of 1 min, the moment of the beginning of the perturbation at AAE coincides with the beginning of the magnetic pulse at high-latitude stations with an accuracy of 1− 2 min. If we assume that ΔX is somehow caused by changes in the MMP, we obtain an estimate of the variation propagation time in the corresponding component of the MMP in the transition layer of ~ 4− 5 min, which agrees with the results of numerical modeling by Samsonov et al. [2006].

From Fig. 4 shows that the variation of any of the presented parameters (except for the solar wind pressure) can be considered as a potential candidate for the trigger of a magnetic pulse.

Further studies have shown that not all parameters of the interplanetary medium can be the cause of a magnetic pulse.

4.1 Role of interplanetary medium parameters in triggering magnetic pulses

Solar wind pressure pulse. Let us dwell on this parameter in more detail, since a number of authors believe that the sudden compression of the diurnal magnetosphere ([Friis-Christensen et al., 1988]; [Sibeck, 1990]; [Vorobyev et al., 1993]; [Yahnin et al., 1995]; [Kim et al., 2017]) leads to the generation of pulses. In [Yahnin et al., 1995] it is noted, in particular, that sometimes magnetic pulses are observed without global SI features. To these signs, the authors include strengthening of rashes, changes in ionospheric conductivity, and bursts of geomagnetic activity in the ELF and VLF bands. In the cited work, the presence/absence of signs of globality was not investigated. The case described in detail in [Kim et al., 2017] has signs of globality. The response of magnetospheres to SI was multifaceted and manifested in rashes and wave activity in the Hertz range. The authors also found a response to SI at thermospheric heights.

For each event, we analyzed the magnetograms of the low-latitude stations Addis Ababa (AAE), Alibag (ABG), and Hermanus (HER). At these latitudes, the solar wind pressure pulse manifests itself as a step-like increase of the geomagnetic *X*-component with a typical value of ~ 40 nTL (see, for example, [Safargaleev et al., 2002]). We consider this indicator as a necessary sign of the SI globalization. The appearance of the signs listed in [Yahnin et al., 1995] is to a large extent determined by the state of the inner magnetosphere (in the literature - "preparedness" of the magnetosphere).

In the auroral zone, the response of the *X* component to SI also has the form of a step, reflecting the compression of the magnetic field, but the step is additionally superimposed by pulsations of the *Pc5* range (in the literature - $P_{SI}5$). Despite the fact that periodicity in the close range is also detected in the magnetic pulse, no significant signs of SI or SC could be detected at equatorial stations. If in the situations when the increase of the *X* component was distinguishable against the background of fluctuations, this increase was no more than 15 nT (see the example in Fig. 5*a*).

Fig. 5.

As follows from Table 2 (column 4), insignificant but detectable to the naked eye step-like pressure changes sometimes occurred on the WIND satellite. However, some of them, being, recalculated at the shock front, did not precede the pulse, but were observed after its onset. Examples of such events are shown in the upper panels of Fig. 5*a, b*.

The result does not agree with the results of a large number of earlier works (see, for example, [Yahnin et al., 1995] and references therein), where it was shown that SIs are the most probable triggers of MIEs. In this connection, we will mention the work of Konik et al., [1994], where it was shown that the vast majority of magnetic pulses occur against the background of rapid changes in the MIE components. The result does not unconditionally exclude SI as a trigger of

impulses, since Moretto et al., 1997, pointed out the existence of at least two different classes of TCVs differing in their generation mechanisms.

Variation of the *Vx*-component of the solar wind speed and the *Bx*-component of the MMP. The nature of the variation of these parameters is summarized in Table 2 (columns 6 and 7). It can be seen that in ~23% of cases *Vx* practically does not change (more precisely, it changes at the level of fluctuations), in~ 47% of cases *Vx* increases, and in ~30% of cases it decreases. The argument for excluding this parameter from the list of possible candidates for launching a magnetic pulse is not the variation's diverse nature (increase or decrease in velocity), but the lag relative to the start of the pulse. In column 6, such events are marked with * and account for ~ 23% of all events. The above is also demonstrated by the example in Fig. 5 *a, b* (second panel from the top).

The *Bx*-component of the MMP changes more systematically - in 19 cases out of 22 *Bx* grows into the region of positive values. At the same time, in 11 cases (50%) *Bx* passes through zero values. In the remaining cases, *Bx* remains in the zone of either negative or positive values when changing. As for *Vx*, the argument to question the role of *Bx* in the initiation of the magnetic pulse is the discrepancy between the time of the pulse onset and the moment of the *Bx* variation onset at the frontal point of the shock front (events Nos. 4, 7, and 8 in Table 2*,* Fig. 5 *a, b*).

We cannot explain the *Vx* and *Bx* delays by inaccurate calculation of the propagation time from the satellite to the shock front, since the other two MMP components, whose variations begin before the magnetic pulse, were measured on the same satellite.

Variations of the *By*- and *Bz*-components of the MMP as the most likely trigger of magnetic pulses. Above, the pressure and velocity of the solar wind and the Bx-component of the MMP were excluded from the list of candidates for triggering a magnetic pulse. The reason is that the variation of these parameters, with which a magnetic pulse could be associated, began after the pulse had already started. The nature of the variation of the remaining two parameters is summarized in Table 2 (columns 8 and 9).

In all cases considered, the *Bz*-component varied. The variations had different amplitude and sign, but, unlike *Vx* and *Bx*, the variations in the *Bz*-component began several minutes before the onset of the magnetic pulse (see examples in Fig. 5, third panel from the bottom). The *By*-component behaved in approximately the same way. Two cases (nos. 9 and 16 in Table 2), when the magnetic pulse began against a background of smoothly decreasing *By*, are an exception. Since in this case distinct variations of the *Bz* component took place before the impulse, both these components remain in the list of trigger candidates. The above is illustrated by the example in Fig. *5a* (fourth panel from the top).

The result is consistent with the results of a statistical study by Konik et al. [1994], which showed that 50− 70% of magnetic pulse events are associated with variations of the *By*- and *Bz*-components of the MMP. Previously, Friis-Christensen et al, [1988] also associated the generation of magnetic pulses (in the form of TCV) with variations in these two components.

5. DISCUSSION

5.1 Ionospheric and longitudinal magnetic pulse currents. Generalization

In all situations studied, the magnetic pulse at high latitudes began as a positive deflection, while at lower latitudes the initial deflection was negative. That is, at high latitudes the pulse was caused by an eastward current amplification, while at lower latitudes it was caused by a westward current amplification. In the region where the equivalent ionospheric current changes direction from eastward to westward, the sole of the longitudinal current flowing into the ionosphere should be located. On 2D maps of the equivalent ionospheric current calculated using the ECLAT program, the trace of the localized longitudinal current flowing into the ionosphere is associated with the center of the current vortex twisted clockwise.

We assume that the magnetic pulse is a product of approximately simultaneous intensification of the eastern and western jets, caused by the intensification or appearance of the localized inflow longitudinal current. In all events presented in this paper, the perturbation of the longitudinal current occurred in the depth of the magnetosphere. The result may imply that the magnetic pulse is not a consequence of a direct interaction between the solar wind inhomogeneity and the magnetopause such as reconnection or the development of a Kelvin-Helmholtz instability at the inner boundary of the *llbl*.

5.2 Scenario of magnetic pulse generation

Based on the generally accepted view that an Alvenov wave is a longitudinal current wave (see, e.g., [Lyatsky and Maltsev, 1983]), we believe that the appearance of the longitudinal current, which is a mediating source of the magnetic pulse, is associated with the generation of an Alvenov wave. Below we present a possible step-by-step scenario in which an Alvenov wave is generated within the magnetosphere in a localized region in response to changes in the MMP. The scenario is based on three theoretical results obtained earlier by other authors.

At the first stage, getting into the transition region between the shock wave and the magnetopause, the MMP variations are transformed into plasma pressure variations. This can occur in the magnetic barrier region, where variations of the magnetic field and plasma concentration (plasma pressure) are interrelated. This qualitative reasoning is supported by the results of numerical simulations ([Lin et al., 1996]). Let us also note the work of Eastwood et al. [2008], where a phenomenon known in the literature as *hot flow anomalies* (HFA) is considered as a possible cause of pressure variations in the transition region in the absence of such variations

in the solar wind. The authors propose to associate with these variations a short-term negative variation of the magnetic field at the ground-based observatory network of the THEMIS project (Fig. 5 in the cited paper), calling it a magnetic pulse. The magnetic pulses considered in our study have a different shape and, unlike the work of Eastwood et al. [2008], the study does not have the character of a case study.

At the second stage, pressure variations, similar to SI, affect the magnetopause, as a result of which the magnetopause becomes a source of secondary waves of magnetosonic type of complex structure but small amplitude.

At the third stage, the shape of the magnetopause is "included" in the process. According to Leonovich and Kozlov [2020], the magnetopause, due to its shape, can act as a collecting lens, amplifying the secondary waves or their effect in the "focus" located inside the daytime magnetosphere. Under the influence of the external environment, the shape of the magnetopause changes, and the position and size of the focus change.

At the fourth stage, the complex wave (coupling of magnetosonic and Alvenov modes) propagates inside the magnetosphere. According to the theory of the magnetospheric Alvenov resonator, MHD perturbations from external regions are transformed into Alvenov oscillations in the process of propagation deep into the magnetosphere. The process of transformation of oscillations is most effective at geomagnetic latitude, where the frequency of the external source coincides with the local frequency of the natural oscillations of the geomagnetic force line (see, for example, [Pilipenko, 2006 and references therein]). In Leonovich and Mazur [1989], the transformation of a magnetosonic wave into an Alvenov wave was studied with respect to SI events. The transformation occurs for both monochromatic and broadband external exciter shapes.

This theoretical result about the transformation of a magnetosonic wave into an Alvenov wave was used by the authors to explain the $P_{SI}5$ pulsations, which are the response of the magnetosphere to SI. If the transformation region is in the "focus" of the magnetopause, the pumping effect will be noticeable.

In the model of Lühr et al. (1996), the transformation of a fast compressional wave mode into an Alven wave occurs on a density gradient, which is assumed to exist in *llbl*. According to our study, the source of MIEs is deeper in the magnetosphere than *llbl*.

The results of [Pilipenko et al., 2021] agree well with our proposed scenario). Observations at conjugate points showed that the TCV is excited by a magnetospheric current generator. The current generator mode corresponds to resonant oscillations in the magnetospheric Alvenov resonator. Such a resonant response to a magnetosonic pulse can indeed occur deep in the magnetosphere and is observed as MIEs/TCV.

Note that the phenomena investigated in this work are not pulses in the traditional sense of the word, but represent a tsunami of damped oscillations. The bipolar character of magnetic pulses was emphasized, in particular, in Vorobyev et al. [1997]. The authors explained this feature by the motion of current vortices. Despite the fact that isolated events were selected for this study, they were not characterized by a distinct onset, which, together with the relatively small temporal resolution of the magnetic data and the lack of a sufficient number of stations at the latitude where the vortex center was located, made it difficult to investigate the question of its motion. We believe that the pulsation form of the pulse could be due to the bouncing of the Alven wave between the conjugate ionospheres.

6. CONCLUSION

Magnetic impulses (MI or *magnetic impulse events*, MIEs) are a daytime high-latitude phenomenon in the form of an isolated tsunami of damped pulsations in the *X*-component of the geomagnetic field consisting of 1− 3 bursts with a period of 8− 12 min. We considered 22 cases of magnetic pulses whose current system consisted of multidirectional ionospheric currents - eastward in the high-latitude part of the Scandinavian IMAGE magnetometer network and westward at stations located to the south. On two-dimensional maps of the distribution of equivalent ionospheric currents, the current system had the form of a clockwise swirling vortex, in the poleward part of which the ionospheric currents flowed predominantly eastward and in the southern part - westward.

For 8 cases, data were available on the ejected particles of DMSP satellites flying over the high-latitude part of the IMAGE network during, immediately before or immediately after the magnetic pulse. From these data, we determined the approximate position of the vortex center relative to the boundaries of the magnetospheric domains. Considering the longitudinal current flowing into the vortex center as mediated by the source of the magnetic pulse, it is shown that the source of the magnetic pulse is either in the central plasma layer, *cps*, or in the boundary plasma layer, *bps*. This means that the previously proposed explanations of magnetic pulses by sporadic reconnection, surface waves at the magnetopause, or Kelvin-Helmholtz instability at the inner boundary of the low-latitude boundary layer, *llbl*, do not agree with the observations. The result is consistent with the results of some case study format studies (see, e.g., [Yahnin et al., 1997]), thus extending the statistics on this issue.

All 22 cases of MIEs were analyzed in the context of the interplanetary situation. According to the results of the analysis, sudden impulses (SI), solar wind speed variations, and *Bx* - *components of* MIEs were excluded from the list of possible candidates for launching MIEs. The result obtained, excluding SI and pointing to variations of the *By*- and *Bz*-components as the most

likely trigger of MIEs, is consistent with the results of other studies (see, for example, Konik et al. [1994]), thus also extending the statistics on this issue.

A step-by-step scenario of magnetic pulse generation by the longitudinal current of an Alvenov wave is proposed. According to the scenario, MMP variations passing through the region between the shock wave and the magnetopause generate plasma pressure variations. The pressure variations affect the magnetopause in a manner similar to SI phenomena, resulting in the magnetopause becoming a source of weak mixed-type secondary waves. The shape of the magnetopause resembles a collecting lens, at the focus of which the secondary waves are amplified. If the magnetospheric section, where the energy of the mixed wave is "pumped" into the Alvenov mode (the possibility of transforming a magnetosonic wave into an Alvenov wave was discussed earlier in relation to the generation of $P_{SI}5$ pulsations), the transformation will lead to the appearance of a longitudinal current. The vortex of ionospheric equivalent current caused by the appearance of the longitudinal current will create a tsunami of damped pulsations on the Earth's surface− magnetic pulse.

ACKNOWLEDGEMENTS

The author thanks Newell P.T. (Johns Hopkins University, APL, Laurel, Maryland, US) for preparing and posting on the Internet the position of auroral rash boundaries from DMSP satellite observations. The IMAGE network data are available on the web site (https://space.fmi.fi/MIRACLE). Data of low-latitude stations AAE, ABG and HER are taken from the INTERMAGNET world database (https://imag-data.bgs.ac.uk/GIN_V1). The position of satellites was determined using the on-line procedure *SSC 4D Orbit Viewer* (https://sscweb.gsfc.nasa.gov). Geomagnetic latitude and local time were calculated by the on-line program VITMO Model (https://omniweb.gsfc.nasa.gov/vitmo/cgm.html).

FUNDING

The work was carried out with the financial support of the state assignment (state registration number 1021100714196-5).

REFERENCES

1. *Vorobyov V.G., Zverev V.L., Starkov G.V.* Geomagnetic pulses in the daytime high-latitude region: main morphological characteristics and connection with the dynamics of daytime auroras // Geomagnetism and Aeronomy. V. 33. P. 69−79. 1993.

2. *Vorobyov V.G., Zverev V.L.* Morphological features of moving current eddies // Geomagnetism and Aeronomy. V. 35. No. 5. P. 35−43. 1997

3. *Lyatsky V.B., Maltsev Yu.P.* Magnetospheric-ionospheric interaction. Moscow: Nauka, 192 p. 1983.

4. *Pilipenko V.A.* Resonance effects of ultra-low-frequency wave fields in near-Earth space // Abstract of a Ph.D. diss. in physics and mathematics. Moscow: Publishing House of the Institute of Physics of the Earth, Russian Academy of Sciences, 33 p. 2006.

5. *Amm O., Engebretson M. J., Hughes T., Newitt L., Viljanen A., Watermann J.* A traveling convection vortex event study: Instantaneous ionospheric equivalent currents, estimation of fieldaligned currents, and the role of induced currents // J. Geophys. Res. V. 107. 1334. 2002. https://doi.org/10.1029/2002JA009472.

6. *Beaujardiere, O. de la, Watermann J., Newell P., Rich F.* Relationship between Birkeland current regions, particle precipitation, and electric field // J. Geophys. Res. V. 98. P. 711−7720. 1993. https://doi.org/10.1029/92JA02005.

7. *Bering III E. A., Lanzerotti L. J., Benbrook J. R., Lin Z.-M.* Solar wind properties observed during high-latitude impulsive perturbation events // Geophys. Res. Lett. V. 17. P. 579−582. 1990. https://doi.org/10.1029/GL017i005p00579.

8. *Clauer C. R., Ridley A. J., Sitar R. J., Singer H. J., Rodger A. S., Friis-Christensen E., Papitashvili V. O.* Field line resonant pulsations associated with a strong dayside ionospheric shear convection flow reversal // J. Geophys. Res. V. 102. P. 4585 – 4596. 1997. https://doi.org/10.1029/96JA02929.

9. *Eastwood J. P., Sibeck D. G., Angelopoulos V., Phan T. D., Bale S. D., McFadden J. P., et al.* THEMIS observations of a hot flow anomaly: Solar wind, magnetosheath, and ground-based measurements // Geophys. Res. Lett. V. 35. N 17. 2008. https://doi.org/10.1029/2008GL033475.

10. *Friis-Christensen E.; McHenry M. A., Clauer C. R., Vennerstrøm S.* Ionospheric traveling convection vortices observed near the polar cleft: A triggered response to sudden changes in the solar wind // Geophys. Res. Lett. V. 15. P. 253–256. 1998. https://doi.org/10.1029/GL015i003p00253.

11. *Goertz C. K., Nielsen E., Korth A., Glassmeier K. H., Haldoupis C., Hoeg P., Hayward D.* Observations of a possible ground signature of flux transfer events // J. Geophys. Res. V. 90. P. 4069–4078. 1985. https://doi.org/10.1029/JA090iA05p04069.

12. *Kim H., Lessard M.R., Jones S.L. et al.* Simultaneous observations of traveling convection vortices: Ionosphere-thermosphere coupling // J. Geophys. Res. V. 122. P. 4943–4959. 2017. https://doi.org/10.1002/2017JA023904.

13. *Konik R. M., Lanzerotti L. J., Wolfe A., Maclennan C. G., Venkatesan D.* Cusp latitude magnetic impulse events, 2, Interplanetary magnetic field and solar wind conditions // J. Geophys. Res. V. 99. P. 14831−14853. 1994. https://doi.org/10.1029/93JA03241.

14. *Lanzerotti L. J., Lee L. C., Maclennan C. G., Wolfe A. and Medford L. V.* Possible evidence of flux transfer events in the polar ionosphere // Geophys. Res. Lett. 13. P. 1089−1092.1986. https://doi.org/10.1029/GL013i011p01089

15. *Leonovich A. S., Mazur V. A.* Resonance excitation of standing Alfven waves in an axisymmetric magnetosphere (nonstationary oscillations) // Planet. Space *Sci.* V. 37. P. 1109–1116. 1989. https://doi.org/10.1016/0032-0633(89)90082-2.

16. *Leonovich A. S., Kozlov D. A.* Focusing of fast magnetosonic waves in the dayside magnetosphere // J. Geophys. Res. V. 125. e2020JA027925. 2020. https://doi.org/10.1029/2020JA027925.

17. *Lin Y., Swift D. W., Lee L. C.* Simulation of pressure pulses in the bow shock and magnetosheath driven by variations in interplanetary magnetic field direction // J. Geophys. Res. V. 101. P. 2725−27269. 1996. https://doi.org/10.1029/96JA02733.

18. *Lühr H., Lockwood M., Sandholt P. E., Hansen T. L., Moretto T.* Multi-instrument ground-based observations of a travelling convection vortices event // Ann. Geophys. V. 1. P. 162−181. 1996. https://doi.org/10.1007/s00585-996-0162-z

19. *Moretto T., Friis-Christensen E.; Lühr H., Zesta E*. Global perspective of ionospheric traveling convection vortices: Case studies of two Geospace Environmental Modeling events // J. Geophys. Res. V. 102. P. 11597–11610. 1997. https://doi.org/10.1029/97JA00324

20. *Moretto T., Sibeck D., Watermann J.* Occurrence statistics of magnetic impulsive events // Annales Geophysicae. V. 22. P. 585−602. 2004. https://doi.org/10.5194/angeo-22-585-2004.

21. *Newell P.T., Wing S., Meng C-I., Sigilitto V.* The auroral oval position, structure and intensity of precipitation from 1984 onward: an automated on-line base // J. Geophys. Res. V. 96. P. 5877−5882. 1991. https://doi.org/10.1029/90JA02450.

22. *Newell P. T., Meng C.-I.* Mapping the dayside ionosphere to the magnetosphere according to particle precipitation characteristics // Geophys. Res. Lett. V.19. P. 609−612. 1992. https://doi.org/10.1029/92GL00404.

23. *Palin L., Opgenoorth H. J., Årgen J., et al.* Modulation of the substorm current wedge by bursty bulk flows: 8 September 2002 – Revisited // J. Geophys. Res. V. 121. P. 4466–4482. 2016. https://doi.org/10.1002/2015JA022262.

24. *Pilipenko V.A., Engebretson M.J., Hartinger M.D, Fedorov E.N., Coyle S.*, Electromagnetic fields of magnetospheric disturbances in the conjugate ionospheres: Current/voltage dichotomy / Cross-Scale Coupling and Energy Transfer in the Magnetosphere-Ionosphere-Thermosphere System, ed. by T. Nishimura, O. Verkhoglyadova, and Y. Deng, Elsevier B.V. Amsterdam. 357-440. 2021. https://doi.org/10.1016/B978-0-12-821366-7.00005-6.

25. *Ridley A. J.* Estimations of the uncertainty in timing the relationship between magnetospheric and solar wind processes // J. Atmos. Solar-Terr. Phys. V. 62. P. 757–771. 2000. https://doi.org/10.1016/S1364-6826(00)00057-2.

26. *Safargaleev V., Kangas J., Kozlovsky A., Vasilyev A.* Burst of ULF noise excited by sudden changes of solar wind dynamic pressure // Ann. Geophys. V.20. P. 1751–1761. 2002. https://doi.org/10.5194/angeo-20-1751-2002.

27. *Samsonov A. A., Nemeček Z., Šafránkova J.* Numerical MHD modeling of propagation of interplanetary shock through the magnetosheath // J. Geophys. Res. V. 111. A08210. 2006. https://doi.org/10.1029/2005JA011537.

28. *Sibeck D. G.* A model for the transient magnetospheric response to sudden solar wind dynamic pressure variations // J. Geophys. Res. V. 95. P. 3755 – 3771.1990. https://doi.org/10.1029/JA095iA04p03755.

29. *Sibeck D. G.* Transient events in the outer magnetosphere: Boundary waves or flux transfer events? // J. Geophys. Res. V. 97. 4009–4026. 1992. https://doi.org/10.1029/91JA03017

30. *Sibeck D.G., Trivedi N.B., Zesta E., Decker R.B., Singer H.J., Szabo A., Tachihara H., Watermann J.* Pressure pulse interaction with the magnetosphere and ionosphere // J. Geophys. Res. V. 108. 1095. 2003. https://doi.org/10.1029/2002JA009675.

31. *Vorobjev V.G., Yagodkina O.I. and Zverev V.L.* Morphological features of bipolar magnetic impulsive events and associated interplanetary medium signatures. // J. Geophys. Res. V. 104. P. 4595−4608. 1999. https://doi.org/10.1029/1998JA900042.

32. *Yahnin A., Titova E., Lubchich A., Bösinger T., Manninen J., Turunen T., Hansen T., Troshichev O., Kotikov A.* Dayside high latitude magnetic impulsive events: their characteristics and relationship to sudden impulses // J. Atmos. Solar-Terr. Phys. V. 57. P. 1569–1582. 1995. https://doi.org/10.1016/0021-9169(95)00090-O.

33. *Yahnin A.G., Vorobjev V.G., Bösinger T., Rasinkangas R., Sibeck D.G., Newell P.T.* On the source region of traveling convection vortices // Geophys. Res. Lett. V. 24. P. 237–240. 1997. https://doi.org/10.1029/96GL03969.

Table 1. Coordinates of magnetic stations

Code	Observatory	Geographic coordinates		Geomagnetic latitude,° N	MLT, h
		latitude,° N	longitude,° E		
NAL	Ny Ålesund	78.92	11.95	75.25	UT+2.7
LYR	Longyerbyen	78.20	15.82	75.12	UT+2.8

HOR	Hornsund	77.00	15.60	74.13	UT+2.6
HOP	Hopen Island	76.51	25.01	73.06	UT+2.9
BJN	Bear Island	74.50	19.20	71.83	UT+2.7
SOR	Sørøya	70.54	22.22	67.70	UT+2.7
SOD	Sodankylä	67.37	26.63	63.92	UT+2.3
NUR	Nurmijärvi	60.50	24.65	56.89	UT+1.8
ABG	Alibag	18.64	72.87	10.69	
AAE	Addis Ababa	9.03	38.77	5.4	
HER	Hermanus	-34.42	19.23	34.03	

Table 2. Magnetic pulses and parameters of the interplanetary medium

№	dd/mm/yyyy	UT	Δ*P*, nPa	ΔX, nTl	ΔVx, %	MMP			domain
						Bx	*By*	*Bz*	
1	2	3	4	5	6	7	8	9	10
1	21/04/2010	06:46	~0	4	+8*	5/2	-2.6/-4	0/-4	*cps*
2	24/04/2010	08:45	~0	1.5	+8	-4/1	0.5/4.5	-1/1	*cps*
3	10/01/2011	08:16	~0	~1	-3	-2/2	0/-2	-3/3	*cps*
4	20/01/2011	08:42	0.35	3.5	+4*	-3/1*	2/0	-1/1.7	*bps/cps*
5	15/02/2011	06:54	~0	~7	+9	-5/1	3/1	2/6	*bps/cps*
6	04/06/2011	07:51	0.4	~5	~0	2/3	0.5/-2.5	-3/1	*cps*
7	05/03/2013	06:09	~0	2	+3	3/-1*	-0.5/-2	1/-1	*bps/cps*
8	18/10/2014	07:37	-	~2	-2*	0/-2.5*	4/1	2/0	*bps*
9	06/01/2010	06:07	0.25	13**	-5	0/2. 5	X	4/-2	
10	29/01/2010	05:05	1.1	13	~0	-1/2.5	2.2/4	3/0	
11	17/01/2011	08:38	0.5	~2	+6*	-4.5/-3	0/2.5	-1/0	
12	26/08/2011	06:31	~0	~1	-7	0/4	-4/0	-1/1	
13	07/11/2011	06:07	0.8	0	~0	0/1	0/-3	1/3	
14	08/02/2012	06:05	~0	~1	-3	-3/1	0/-3	1.5/4	
15	29/02/2012	07:22	1.5	~8	+3	-5/1	2/4	2/-4	
16	16/02/2013	07:42	0.2	0	~0	-2.5/-2	X	0/-2	
17	03/03/2013	08:37	~0	10	+9*	4.5/2.5	0/-4	-2/1	
18	16/10/2013	08:45	0.4	3	+3	-3/-1.5	-1.2	-1.5/1	
19	18/10/2013	06:05	~0	~0	+4	-3.5/-2	-1/3	1/0	
20	28/10/2013	09:11	0.4	10	~0	0.5/1.2	-0/-4.7	4.5/0	
21	20/04/2014	07:28	0.5	~0	-2	-5/-2	1/0	1/4	
22	06/10/2014	06:33	-	2	+2.5	3/4	-3/0	0.5/2.5	

Note: The symbol * refers to a parameter whose onset of variation does not agree with the onset of the magnetic pulse. The symbol ** denotes the pressure variation in eV/cm^3

Figure captions

Fig. 1. (*a*)− Magnetic pulse on the chain of IMAGE stations (highlighted in gray). The moment of passage of the F16 satellite is shown by the arrow. (*b*)− 1D distribution of the equivalent ionospheric current showing the dynamics of the east (+) and west (-) currents of the magnetic pulse at meridian 22° E. (*c)*− Vortex character of the equivalent current distribution. The direction of the current is shown by arrows.

Fig. 2. (*a*)− The character of spills along the satellite trajectory with magnetospheric domains indicated three minutes after the start of the pulse. (*b*)− F16 trajectory fragment. The position of the *cps/bps* boundaries is shown with crosses. The *bps* spillout region is shaded in gray. Dashed line - geomagnetic latitude (domain boundaries outside the trajectory). The square is the center of the vortex at meridian 22°E, along which the 1D distribution of the equivalent current in Fig. 1*b* was calculated

Fig. 3. (*a*)− - Counter-phase character of the magnetic field variation. The arrow shows the moment of passage of the F17 satellite over the IMAGE network. (*b*)− Dynamics of the eastern (+) and western (-) magnetic momentum currents at the 22° E meridian. The thin vertical line is the time instant for which the equivalent current map was calculated. (*c*)-Vortex structure with multiple centers on the magnetic pulse equivalent current map. The direction of the current is shown by arrows. (*d*)− Character of the rashes over the observation area from the DMSP F17 data. (*e*)− F17 trajectory fragment. Crosses - reference points for trajectory construction. Squares - position of the vortex center.

Fig. 4. Variations of the interplanetary medium parameters near the frontal point of the shock wave over a time interval including the magnetic pulse observation interval (highlighted in gray, see also Fig. *3a*). From top to bottom: solar wind velocity and pressure, three components of the MMP. Bottom panel: stepwise magnification of the *X* component of the geomagnetic field at the AAE equatorial station.

Fig. 5. Three examples of magnetic pulses (intervals highlighted in gray) in the context of the variation of interplanetary medium parameters at the frontal point of the shock front. From top to bottom: variations in solar wind pressure and velocity, variations in the MMP, magnetograms of IMAGE network stations demonstrating the antiphase character of the magnetic pulse, and variations in the geomagnetic field at equatorial stations.

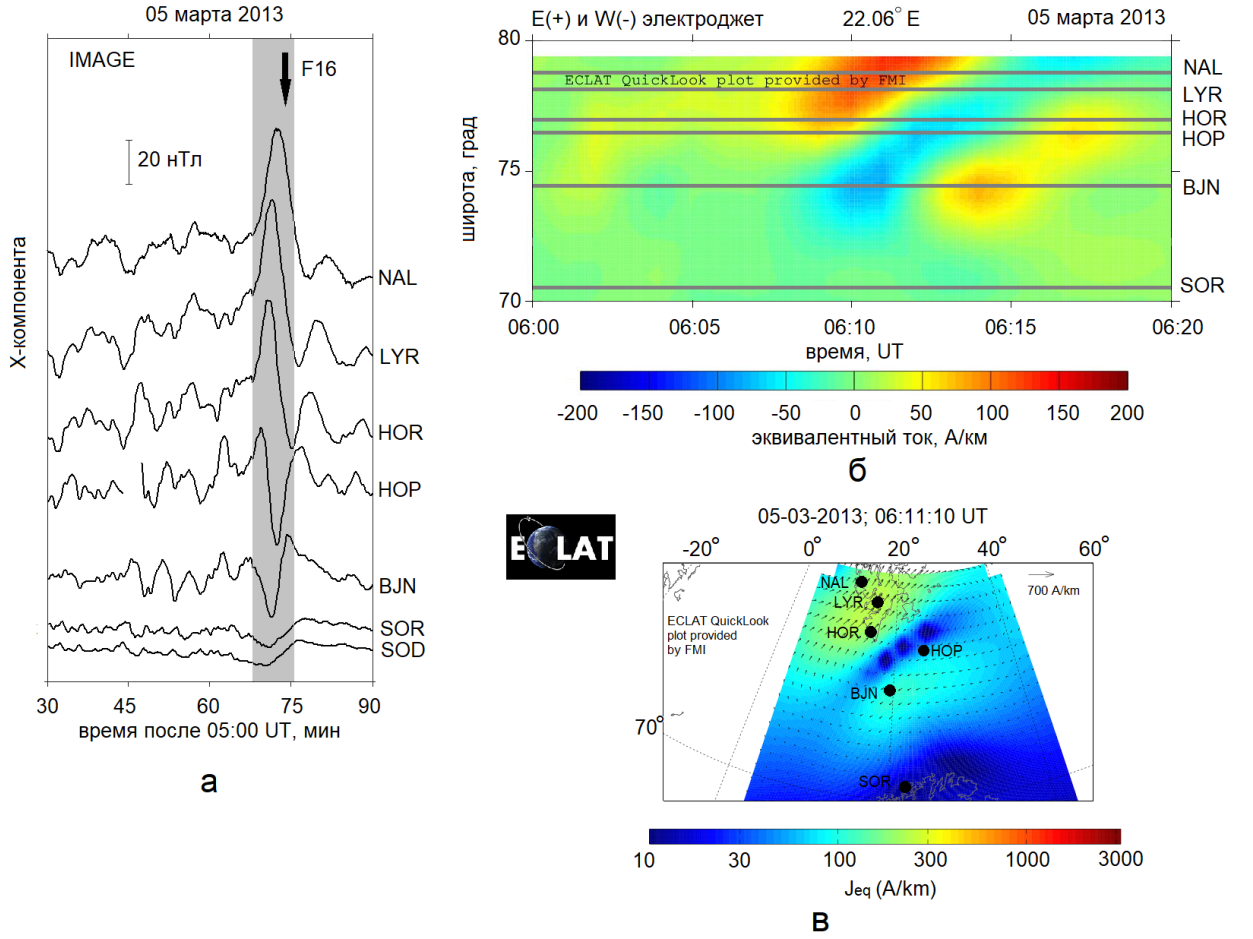
05 марта 2013
IMAGE
F16
20 нТл
X-компонента
NAL
LYR
HOR
HOP
BJN
SOR
SOD
30
45
60
75
90
время после 05:00 UT, мин
а
E(+) и W(-) электроджет
22.06° E
05 марта 2013
ECLAT QuickLook plot provided by FMI
широта, град
80
75
70
06:00
06:05
06:10
06:15
06:20
время, UT
-200
-150
-100
-50
0
50
100
150
200
эквивалентный ток, А/км
б
05-03-2013; 06:11:10 UT
-20°
0°
20°
40°
60°
70°
700 A/km
ECLAT QuickLook plot provided by FMI
10
30
100
300
1000
3000
Jeq (A/km)
в

Fig. 1.

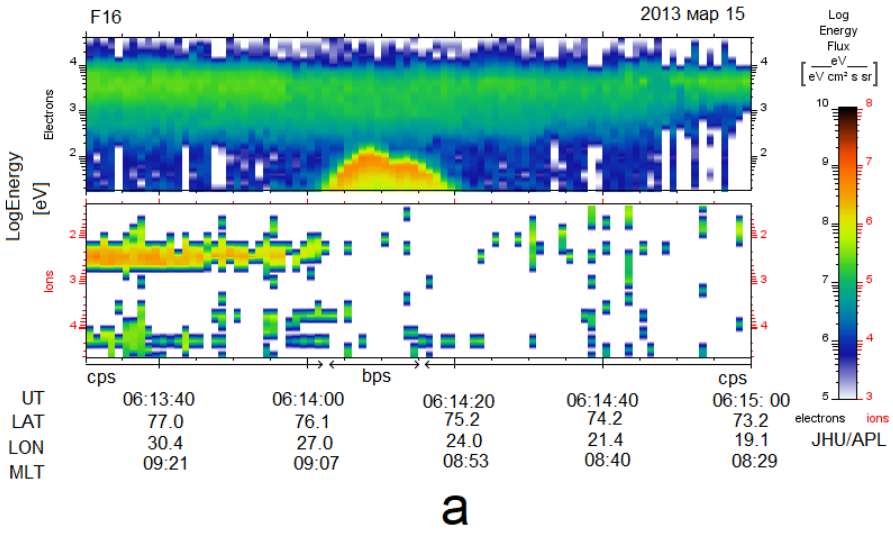
F16
2013 мар 15
Log Energy Flux
LogEnergy [eV]
Electrons
Ions
cps
bps
cps
UT 06:13:40 06:14:00 06:14:20 06:14:40 06:15: 00
LAT 77.0 76.1 75.2 74.2 73.2
LON 30.4 27.0 24.0 21.4 19.1
MLT 09:21 09:07 08:53 08:40 08:29
electrons ions
JHU/APL

а

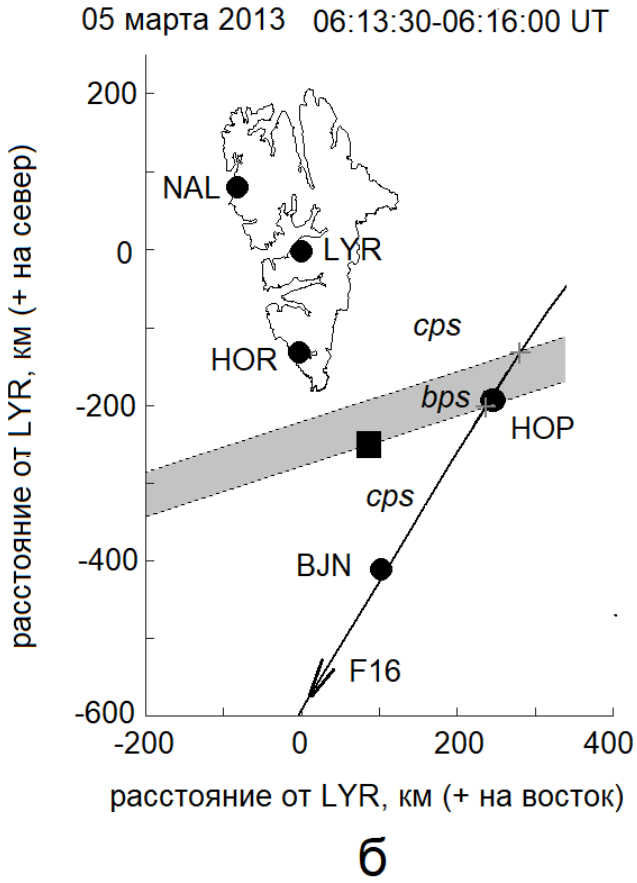
05 марта 2013 06:13:30-06:16:00 UT
NAL
LYR
HOR
cps
bps
HOP
cps
BJN
F16
расстояние от LYR, км (+ на север)
расстояние от LYR, км (+ на восток)

б

Fig. 2.

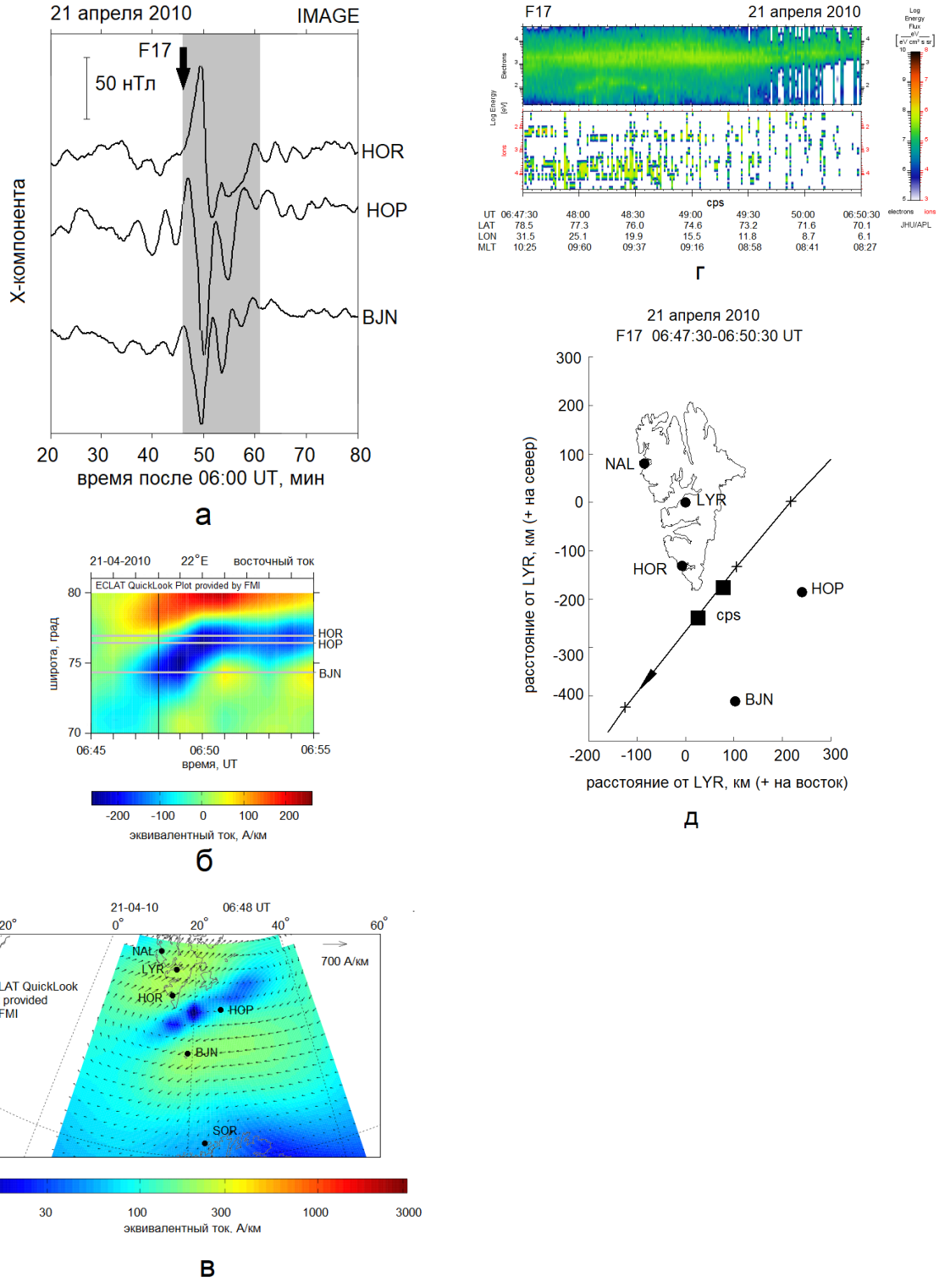
21 апреля 2010
IMAGE
F17
50 нТл
HOR
HOP
BJN
X-компонента
20 30 40 50 60 70 80
время после 06:00 UT, мин
а
21-04-2010
22°E
восточный ток
ECLAT QuickLook Plot provided by FMI
80
75
70
широта, град
HOR
HOP
BJN
06:45
06:50
06:55
время, UT
-200 -100 0 100 200
эквивалентный ток, А/км
б
21-04-10
06:48 UT
-20° 0° 20° 40° 60°
NAL
LYR
HOR
HOP
BJN
SOR
700 А/км
ECLAT QuickLook
plot provided
by FMI
широта
70°
10 30 100 300 1000 3000
эквивалентный ток, А/км
в
F17
21 апреля 2010
Log Energy Flux
Electrons
Log Energy [eV]
Ions
cps
UT 06:47:30 48:00 48:30 49:00 49:30 50:00 06:50:30
LAT 78.5 77.3 76.0 74.6 73.2 71.6 70.1
LON 31.5 25.1 19.9 15.5 11.8 8.7 6.1
MLT 10:25 09:60 09:37 09:16 08:58 08:41 08:27
electrons
ions
JHU/APL
г
21 апреля 2010
F17 06:47:30-06:50:30 UT
300
200
100
0
-100
-200
-300
-400
расстояние от LYR, км (+ на север)
NAL
LYR
HOR
HOP
cps
BJN
-200 -100 0 100 200 300
расстояние от LYR, км (+ на восток)
д

Fig. 3.

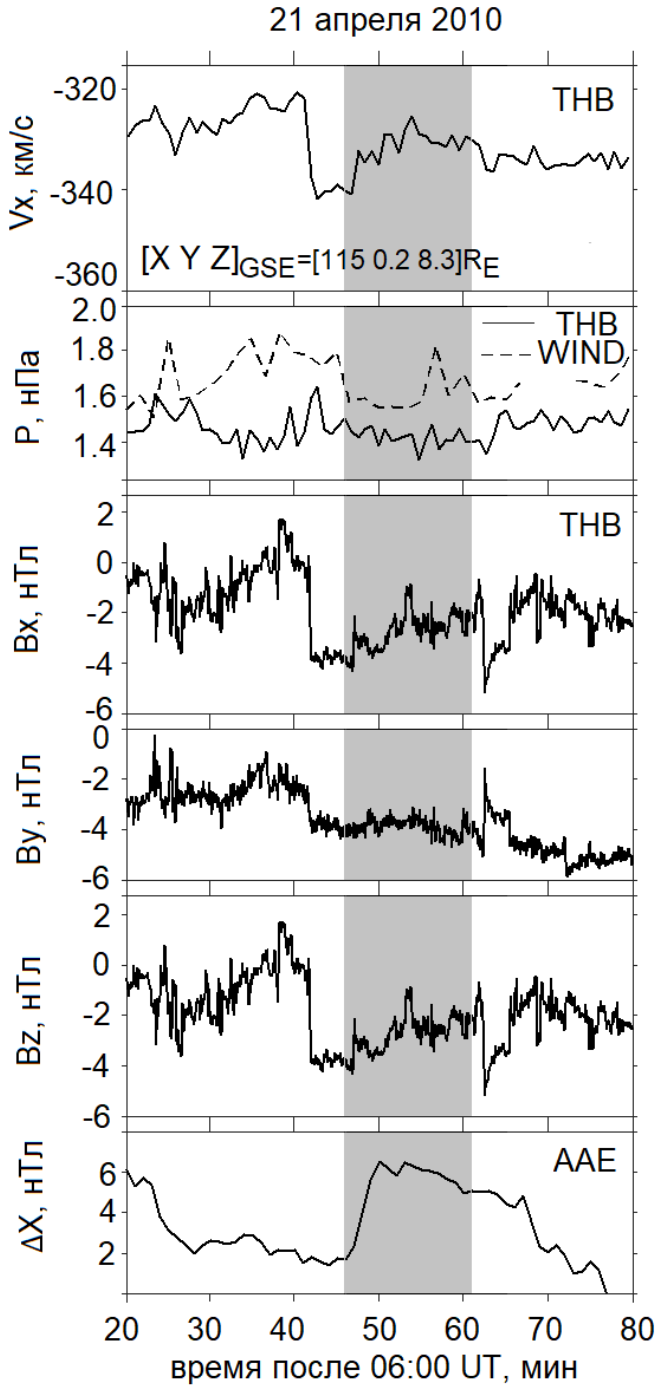
21 апреля 2010
Vx, км/с
-320
-340
-360
THB
[X Y Z]GSE=[115 0.2 8.3]RE
P, нПа
2.0
1.8
1.6
1.4
THB
WIND
Bx, нТл
2
0
-2
-4
-6
THB
By, нТл
0
-2
-4
-6
Bz, нТл
2
0
-2
-4
-6
ΔX, нТл
6
4
2
AAE
20
30
40
50
60
70
80
время после 06:00 UT, мин

Fig. 4.

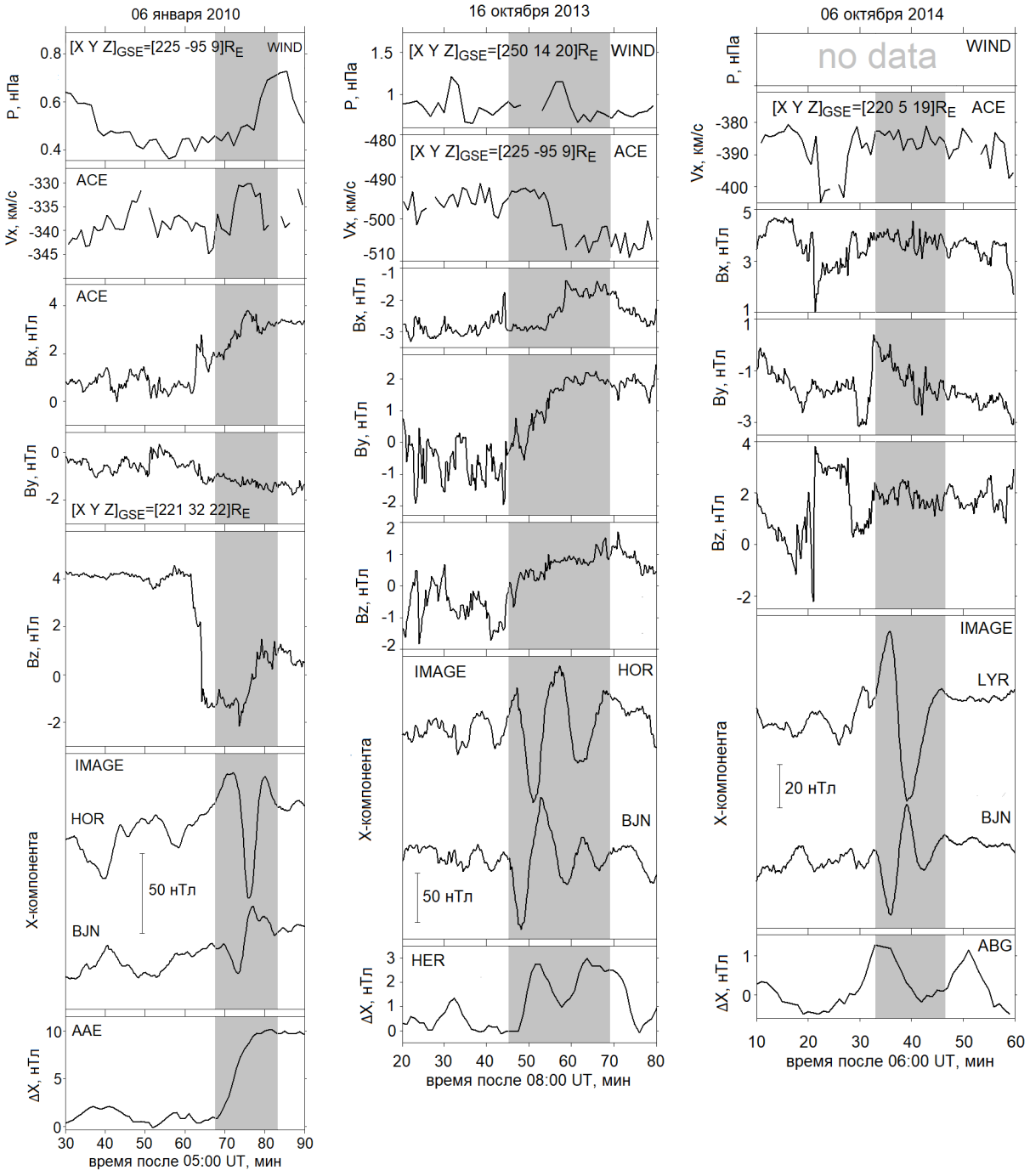
06 января 2010
[X Y Z]GSE=[225 -95 9]RE
WIND
P, нПа
ACE
Vx, км/с
Bx, нТл
By, нТл
[X Y Z]GSE=[221 32 22]RE
Bz, нТл
IMAGE
HOR
50 нТл
BJN
X-компонента
AAE
ΔX, нТл
время после 05:00 UT, мин
a
16 октября 2013
[X Y Z]GSE=[250 14 20]RE
WIND
[X Y Z]GSE=[225 -95 9]RE
ACE
IMAGE
HOR
BJN
50 нТл
HER
время после 08:00 UT, мин
b
06 октября 2014
no data
[X Y Z]GSE=[220 5 19]RE
ACE
IMAGE
LYR
20 нТл
BJN
ABG
время после 06:00 UT, мин
c

Fig. 5.